21st International Symposium on
Mathematical Theory of Networks and Systems
July 7-11, 2014. Groningen, The Netherlands

On the Functional Controllability Using a Geometric Approach together with a Decoupled MPC for Motion Control in Robotino

Daniel Straßberger*, Paolo Mercorelli* and Anthimos Georgiadis*

Abstract— **This paper proposes a functional controller for motion control of the Robotino. The proposed controller takes under consideration a functional decoupling control strategy realized using a geometric approach and the invertibility property of the DC-drives with which the Robotino is equipped. For a given control structure the functional controllability is proven for motion trajectories of class C^3, continuous functions with third derivative also continuous. Horizon, Vertical and Angular motions are considered and once the decoupling between these motions is obtained, a Model Predictive Control (MPC) strategy is used in combination with the inverse DC-drive model. Simulation results using real data of Robotino are shown.**

Index Terms— **Geometric approach; Multivariable systems; Linear systems**
AMS Subject Classification: 14L24; 93C35; 93C05

I. INTRODUCTION

This paper presents a systematic procedure in order to obtain the decoupling controllability between horizontal, vertical and angular motions and their functional controllability. Here, the functional decoupling problem is investigated and roughly speaking, it consists of achieving motion tracking with no error variables transients. To achieve a decoupling effect a feedback control law is needed together with a feed-forward regulator. The functional controllability represents a structural property of the system which must be proven. In this paper a decoulped and functional controller is obtained. The relevance of the motion functional controllability to Robotino control is justified by the necessity of very fast and very precise loops of acceleration control counteracting errors in displacements caused by possible disturbance actions. In the past three decades, research on the geometric approach to dynamic systems theory and control has allowed this approach to become a powerful and a thorough tool for the analysis and synthesis of dynamic systems [1], [2], [3]. Over the same time period, mechanical systems used in industry and developed in research labs have also evolved rapidly. Mobile robotics is a notable case of such evolution. The robotics community has developed sophisticated analysis and control techniques to meet increasing requirements on the control of motions of mechanical systems. These increasing requirements are motivated by higher performance specifications and an increasing number of degrees-of-freedom. References [4] and [5] mark progress in the analysis and synthesis of geometric controller for mechanical systems, and [6] proposes non-interacting force-motion control in robotic manipulation. Reference [7] reports the possibility of parameterising input controlled subspaces to guarantee non-interaction. In [4], a robust decoupling controller using an algebraic state input feedback is presented, while this paper presents a robust decoupling controller using an algebraic output-input feedback. The force/motion control problem has attracted significant attention over last decade in the fields of robotic manipulation and mobile robotics. Approaches exploiting input-output decoupling controllers are found, for instance, in the work [8]. The geometric approach allows very elegant solutions to control problems. Nevertheless, robustness analysis using a linear geometric control offers answers through rank conditions of matrices that are necessary conditions. These conditions are often not constructive conditions. Even though the rank conditions offer simple ”on-off” conditions, it is also possible to measure the robustness. In [4], a robust decoupling controller is obtained using a state input feedback controller. The drawback of this approach consists of a wide sensing structure. In fact, the whole state space should be available and sensed. With the approach proposed in this paper, the robust decoupling is obtained with an output feedback from the contact forces and the joint positions. The goal of this paper is to propose a complete constructive procedure for the design of a decoupling controller. In Robotino case, to achieve a decoupling between Horizontal, Vertical and Angular motions a preselecting field law is needed together with a feed-forward regulator. The paper is organised in the

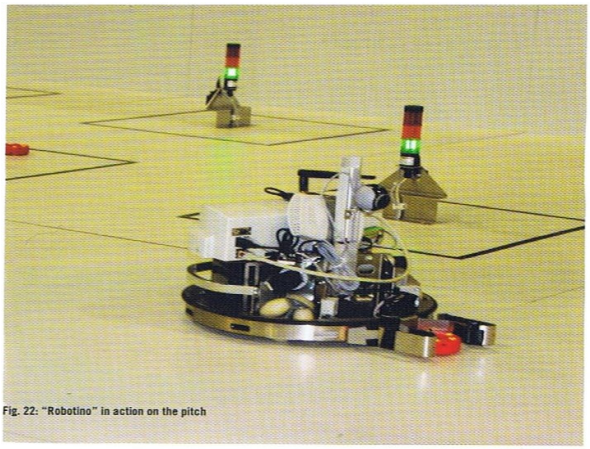

Fig. 1. Robotino in action on the pitch.

*The authors are with the Institute of Product and Process Innovation, Leuphana University of Lueneburg, Volgershall 1, D-21339 Lueneburg, Germany Phone: +49-(0)4131-677-5571, Fax: +49-(0)4131-677-5300. Daniel.Strassberger@stud.leuphana.de, [mercorelli, georgiadis]@uni.leuphana.de

following way: Section II presents a possible model of the Robotino. Section III shows the decoupling strategy using the geometric approach. Section IV presents the functional controllability problem in the case of robotino. Section V is devoted to the derivation of the Model Predictive Control (MPC) strategy. At the end, numerical computer simulations are considering real data of the Robotino are shown.

The main nomenclature
$\mathbf{A}$: state matrix of the mechanical model
$\mathbf{g}(\theta)$: input field of the mechanical model
$\mathbf{T}(\theta)$: decoupling input partition field
$\mathcal{B} = \mathbf{g}(\Theta) \cdot \mathbf{T}(\theta)$: decoupled input matrix of the mechanical model
$\mathcal{B} = \mathrm{im}\mathbf{B}$: image of matrix $\mathbf{B}$
(subspace spanned by the columns of matrix $\mathbf{B}$)
$\mathrm{min}\mathcal{I}(\mathbf{A}, \mathcal{B}) = \sum_{i=0}^{n-1} \mathbf{A}^i \mathrm{im}\mathbf{B}$: minimum $\mathbf{A}$–invariant subspace containing $\mathrm{im}(\mathbf{B})$
$\mathcal{C} = \mathrm{ker}\mathbf{C}$: kernel of matrix $\mathbf{C}$
(subspace spanned by the columns of matrix $\mathbf{C}$)

II. Mechanical and Electrical Model Description

In Fig. 2 a diagram with the representation of the forces in the considered system is shown. If state vector $\mathbf{X}(t)$ is

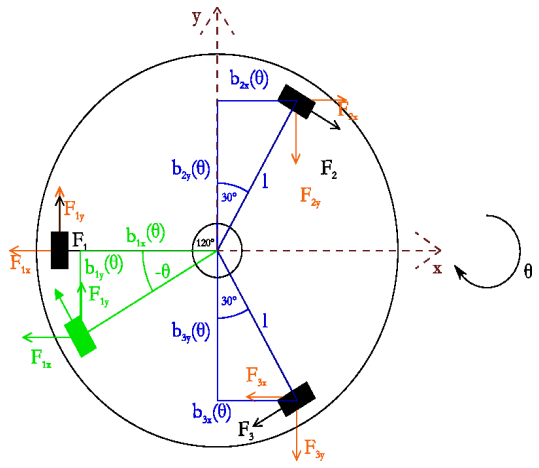

Fig. 2. Mechanical schematic diagram of Robotino.

defined as, $x(t)$ and $y(t)$ positions of the center of mass of the system and its velocities, $\dot{x}(t)$ and $\dot{y}(t)$, moreover considering the angular dynamics with its angular position $\theta(t)$ and its velocity $\dot{\theta}(t)$, then the following system is derived.

$$\begin{cases} \dot{\mathbf{X}}(t) = \mathbf{A}\mathbf{X}(t) + \mathbf{g}(\theta)\mathbf{F}(t) \\ \mathbf{O}(t) = \mathbf{C}\mathbf{X}(t), \end{cases} \tag{1}$$

with

$$\mathbf{X}(t) = \begin{bmatrix} x(t) \\ \dot{x}(t) \\ y(t) \\ \dot{y}(t) \\ \theta(t) \\ \dot{\theta}(t) \end{bmatrix}, \qquad \dot{\mathbf{X}}(t) = \begin{bmatrix} \dot{x}(t) \\ \ddot{x}(t) \\ \dot{y}(t) \\ \ddot{y}(t) \\ \dot{\theta}(t) \\ \ddot{\theta}(t), \end{bmatrix} \tag{2}$$

matrix

$$\mathbf{A} = \begin{bmatrix} 0 & 1 & 0 & 0 & 0 & 0 \\ 0 & -\frac{k_v}{M} & 0 & 0 & 0 & 0 \\ 0 & 0 & 0 & 1 & 0 & 0 \\ 0 & 0 & 0 & -\frac{k_v}{M} & 0 & 0 \\ 0 & 0 & 0 & 0 & 0 & 1 \\ 0 & 0 & 0 & 0 & 0 & -\frac{k_\theta}{J} \end{bmatrix}, \tag{3}$$

which for sake of notation can be written as follows:

$$\mathbf{A} = \begin{bmatrix} \mathbf{A}_{x2\times2} & \mathbf{0}_{2\times2} & \mathbf{0}_{2\times2} \\ \mathbf{0}_{2\times2} & \mathbf{A}_{y2\times2} & \mathbf{0}_{2\times2} \\ \mathbf{0}_{2\times2} & \mathbf{0}_{2\times2} & \mathbf{A}_{\theta2\times2} \end{bmatrix}, \tag{4}$$

where $\mathbf{A}_{x2\times2}$, $\mathbf{A}_{y2\times2}$ and $\mathbf{A}_{\theta2\times2}$ are the minor matrices of $\mathbf{A}$ describing the x, y and θ dynamics of the system. Matrix $\mathbf{C}$ represents the output matrix and can be written in the following way:

$$\mathbf{C} = \begin{bmatrix} 1 & 0 & 0 & 0 & 0 & 0 \\ 0 & 0 & 1 & 0 & 0 & 0 \\ 0 & 0 & 0 & 0 & 1 & 0 \end{bmatrix}, \tag{5}$$

where the following notation is assumed:

$$\mathbf{C}_\mathbf{x} = \begin{bmatrix} 1 & 0 & 0 & 0 & 0 & 0 \end{bmatrix}, \tag{6}$$
$$\mathbf{C}_\mathbf{y} = \begin{bmatrix} 0 & 0 & 1 & 0 & 0 & 0 \end{bmatrix}, \tag{7}$$
$$\mathbf{C}_\theta = \begin{bmatrix} 0 & 0 & 0 & 0 & 1 & 0 \end{bmatrix}. \tag{8}$$

Field $\mathbf{g}(\theta)$ is as follows

$$\mathbf{g}(\theta) = \begin{bmatrix} 0 & 0 & 0 \\ \frac{\sin(\theta)}{M} & \frac{\sin(\frac{2}{3}\pi+\theta)}{M} & -\frac{\sin(\frac{2}{3}\pi-\theta)}{M} \\ 0 & 0 & 0 \\ \frac{\cos(\theta)}{M} & \frac{\cos(\frac{2}{3}\pi+\theta)}{M} & \frac{\cos(\frac{2}{3}\pi-\theta)}{M} \\ 0 & 0 & 0 \\ \frac{\sin(\theta)\cdot l\cdot\sin(\theta)+\cos(\theta)\cdot l\cdot\cos(\theta)}{J} & \frac{\sin(\frac{2}{3}\pi+\theta)\cdot l\cdot\cos(\frac{\pi}{6}+\theta)+\cos(\frac{2}{3}\pi+\theta)\cdot l\cdot\sin(\frac{\pi}{6}+\theta)}{J} & \frac{-\sin(\frac{2}{3}\pi-\theta)\cdot l\cdot-\cos(\frac{\pi}{6}-\theta)+\cos(\frac{2}{3}\pi-\theta)\cdot l\cdot\sin(\frac{\pi}{6}-\theta)}{J} \end{bmatrix} \tag{9}$$

and force input vector signal $\mathbf{F}(t) = \begin{bmatrix} F_1(t) \\ F_2(t) \\ F_3(t) \end{bmatrix}$ in which $F_1(t) = K_m i_1(t)/r$, $F_2(t) = K_m i_2(t)/r$ and $F_3(t) = K_m i_3(t)/r$, where K_m represents the motor constant, r the radius of the wheels and variables $i_1(t)$, $i_2(t)$ and $i_3(t)$ are the currents of the three DC-electrical drives. In fact, the Robotino consists of 3 DC electrical drives that power the three omniwheels. The models of these three DC-drive is reported are below.

$$\begin{bmatrix} \frac{di_1(t)}{dt} \\ \frac{d\omega_1(t)}{dt} \\ \frac{di_2(t)}{dt} \\ \frac{d\omega_2(t)}{dt} \\ \frac{di_3(t)}{dt} \\ \frac{d\omega_3(t)}{dt} \end{bmatrix} = \begin{bmatrix} -\frac{R}{L} & -\frac{K_m}{L} & 0 & 0 & 0 & 0 \\ \frac{K_m}{J} & -\frac{K}{J} & 0 & 0 & 0 & 0 \\ 0 & 0 & -\frac{R}{L} & -\frac{K_m}{L} & 0 & 0 \\ 0 & 0 & \frac{K_m}{J} & -\frac{K}{J} & 0 & 0 \\ 0 & 0 & 0 & 0 & -\frac{R}{L} & -\frac{K_m}{L} \\ 0 & 0 & 0 & 0 & \frac{K_m}{J} & -\frac{K}{J} \end{bmatrix} \cdot$$

$$\begin{bmatrix} i_1(t) \\ \omega_1(t) \\ i_2(t) \\ \omega_2(t) \\ i_3(t) \\ \omega_3(t) \end{bmatrix} + \begin{bmatrix} \frac{1}{L} & 0 & 0 \\ 0 & 0 & 0 \\ 0 & \frac{1}{L} & 0 \\ 0 & 0 & 0 \\ 0 & 0 & \frac{1}{L} \\ 0 & 0 & 0 \end{bmatrix} \cdot \begin{bmatrix} U_{inp_1}(t) \\ U_{inp_2}(t) \\ U_{inp_3}(t) \end{bmatrix}, \quad (10)$$

where $U_{inp_1}(t)$, $U_{inp_2}(t)$ and $U_{inp_3}(t)$ represent the input voltage of the DC-drive, L is the inductance, R is the resistance, J represents the motor inertia factor, K_m is the motor moment and finally K can be seen as the friction factor. This model is important in realising the simulation and is basis for the inverted drive used in the control strategy (see Fig. 3) but is otherwise not explicitly used in the MPC.

III. Design of a decoupling controller

This section describes the design of a decoupling controller with respect to the x-y and θ motions above defined. A geometric approach is used in this analysis. The earliest geometric approaches to decoupling control were due to Basile and Marro ([9], [1]) and to Wonham and Morse ([10], [11], and [3]). Since the geometric relations depend on the rotational position (θ), the forces actuated by the three DC drives needed to move in a certain direction may be difficult to obtain.

Definition 1: A control law for the dynamic system (1) is *decoupling* with respect to the regulated outputs $x(t)$, $y(t)$, and $\theta(t)$, if there exists partitions $F_x(t), F_y(t)$, and $F_\theta(t)$ of the input vector $\mathbf{F}(t)$ such that for zero initial conditions, each input $F_{(\cdot)}(t)$ (with all other inputs, identically zero) only affects the corresponding output $x(t)$, $y(t)$, or $\theta(t)$. □

It it to be shown that there exists a decoupling and stabilizing state feedback field $\mathbf{D}(\theta)$, along with three input partition fields $\mathbf{T}_x(\theta)$, $\mathbf{T}_y(\theta)$, and $\mathbf{T}_\theta(\theta)$ such that, for the dynamic triples

$$\begin{array}{c} (\mathbf{C}_x,\, \mathbf{A} + \mathbf{g}(\theta)\mathbf{D}(\theta),\, \mathbf{g}(\theta)\mathbf{F}_1(t))\,, \\ (\mathbf{C}_y,\, \mathbf{A} + \mathbf{g}(\theta)\mathbf{D}(\theta),\, \mathbf{g}(\theta)\mathbf{F}_2)\,, \\ (\mathbf{C}_\theta,\, \mathbf{A} + \mathbf{g}(\theta)\mathbf{D}(\theta),\, \mathbf{g}(\theta)\mathbf{F}_3(t))\,, \end{array} \quad (11)$$

it holds the following conditions:

$$\mathcal{R}_x(\theta) = \mathsf{min}\mathcal{I}\Big(\mathbf{A} + \mathbf{g}(\theta)\mathbf{D}(\theta),\, \mathbf{g}(\theta)\mathbf{T}_x(\theta)\Big) \subseteq \mathcal{C}_y \cap \mathcal{C}_\theta \;\; \forall\theta, \quad (12)$$

and

$$\mathbf{C}_x\mathcal{R}_x(\theta) = \mathsf{im}(\mathbf{C}_x), \;\; \forall\theta. \quad (13)$$

$$\mathcal{R}_y(\theta) = \mathsf{min}\mathcal{I}\Big(\mathbf{A} + \mathbf{g}(\theta)\mathbf{D}(\theta),\, \mathbf{g}(\theta)\mathbf{T}_y(\theta)\Big) \subseteq \mathcal{C}_x \cap \mathcal{C}_\theta \;\; \forall\theta, \quad (14)$$

and

$$\mathbf{C}_y\mathcal{R}_y(\theta) = \mathsf{im}(\mathbf{C}_y), \;\; \forall\theta. \quad (15)$$

$$\mathcal{R}_\theta(\theta) = \mathsf{min}\mathcal{I}\Big(\mathbf{A} + \mathbf{g}(\theta)\mathbf{D}(\theta),\, \mathbf{g}(\theta)\mathbf{T}_\theta(\theta)\Big) \subseteq \mathcal{C}_x \cap \mathcal{C}_y \;\; \forall\theta, \quad (16)$$

and

$$\mathbf{C}_\theta\mathcal{R}_\theta(\theta) = \mathsf{im}(\mathbf{C}_\theta), \;\; \forall\theta. \quad (17)$$

Here,

$$\mathsf{min}\mathcal{I}(\mathbf{A}, \mathsf{im}(\mathbf{g}(\theta))) = \sum_{i=0}^{n-1} \mathbf{A}^i \mathsf{im}(\mathbf{g}(\theta))$$

is a minimum $\mathbf{A}$–invariant subspace containing $\mathsf{im}(\mathbf{g}(\theta))$ $\forall$ θ. Moreover, the partition fields $\mathbf{T}_x(\theta)$, $\mathbf{T}_y(\theta)$ and $\mathbf{T}_\theta(\theta)$ satisfy the following relationships:

$$\begin{array}{l} \mathsf{im}(\mathbf{g}(\theta) \cdot \mathbf{T}_x(\theta)) = \mathsf{im}(\mathbf{g}(\theta)) \cap \mathcal{R}_x(\theta), \\ \mathsf{im}(\mathbf{g}(\theta) \cdot \mathbf{T}_y(\theta)) = \mathsf{im}(\mathbf{g}(\theta)) \cap \mathcal{R}_y(\theta), \\ \mathsf{im}(\mathbf{g}(\theta) \cdot \mathbf{T}_\theta(\theta)) = \mathsf{im}(\mathbf{g}(\theta)) \cap \mathcal{R}_\theta(\theta). \end{array} \quad (18)$$

The stabilizing field $\mathbf{D}(\theta)$ is such that:

$$(\mathbf{A} + \mathbf{g}(\theta)\mathbf{D}(\theta))\mathcal{R}_x(\theta) \subseteq \mathcal{R}_x(\theta), \quad (19)$$

$$(\mathbf{A} + \mathbf{g}(\theta)\mathbf{D}(\theta))\mathcal{R}_y(\theta) \subseteq \mathcal{R}_y(\theta), \quad (20)$$

and

$$(\mathbf{A} + \mathbf{g}(\theta)\mathbf{D}(\theta))\mathcal{R}_\theta(\theta) \subseteq \mathcal{R}_\theta(\theta). \quad (21)$$

Considering matrix $\mathbf{A}$ defined in (3) it is straightforward to see that this matrix is structurally already decoupled and intrinsically stable, this implies that field $\mathbf{D}(\theta) = \mathbf{0}$ $\forall\theta$. Considering

$$\mathbf{T}(\theta) = [\mathbf{T}_x(\theta), \mathbf{T}_y(\theta), \mathbf{T}_\theta(\theta), \mathbf{T}_c(\theta)],$$

where $\mathbf{T}_c(\theta)$ is defined in a complementary fashion and it is straightforward to show that matrix $\mathbf{T}_c = \mathbf{0}$. In particular, matrix $\mathbf{T}_c$ represents the complementary field partition to the subspaces of x-position, y-position and angular position of the Robotino. The Robotino motion is described using just three variables, therefore partitions $\mathbf{T}_x(\theta), \mathbf{T}_y(\theta), \mathbf{T}_\theta(\theta)$ complete the transformation and thus $\mathbf{T}_c = \mathbf{0}$.

$$\mathsf{im}\mathbf{T}(\theta) = \mathsf{im}[\mathbf{T}_x(\theta), \mathbf{T}_y(\theta), \mathbf{T}_\theta(\theta)] = \mathsf{im}\mathbf{T}_x(\theta) \oplus \mathsf{im}\mathbf{T}_y(\theta) \oplus \mathsf{im}\mathbf{T}_\theta(\theta). \quad (22)$$

Considering the output matrices (6), (7) and (8) corresponding to x-position, y-position and angular position their respective kernels are as follows:

$$\mathcal{C}_x = \mathsf{im}\begin{bmatrix} 0 & 0 & 0 & 0 & 0 \\ -1 & 0 & 0 & 0 & 0 \\ 0 & -1 & 0 & 0 & 0 \\ 0 & 0 & -1 & 0 & 0 \\ 0 & 0 & 0 & -1 & 0 \\ 0 & 0 & 0 & 0 & -1 \end{bmatrix}, \quad (23)$$

$$\mathcal{C}_y = \mathsf{im}\begin{bmatrix} 1 & 0 & 0 & 0 & 0 \\ 0 & -1 & 0 & 0 & 0 \\ 0 & 0 & 0 & 0 & 0 \\ 0 & 0 & -1 & 0 & 0 \\ 0 & 0 & 0 & -1 & 0 \\ 0 & 0 & 0 & 0 & 1 \end{bmatrix}, \quad (24)$$

$$\mathcal{C}_\theta = \mathsf{im}\begin{bmatrix} 1 & 0 & 0 & 0 & 0 \\ 0 & 1 & 0 & 0 & 0 \\ 0 & 0 & 1 & 0 & 0 \\ 0 & 0 & 0 & -1 & 0 \\ 0 & 0 & 0 & 0 & 0 \\ 0 & 0 & 0 & 0 & 1 \end{bmatrix}. \quad (25)$$

According to relation (9) it is straightforward to observe that the following three equations hold $\forall\ \theta$;

$$\mathsf{im}(\mathbf{g}(\theta)) \cap \left(\mathcal{C}_x \cap \mathcal{C}_y\right) \neq \mathbf{0}, \quad (26)$$

$$\mathsf{im}(\mathbf{g}(\theta)) \cap \left(\mathcal{C}_x \cap \mathcal{C}_\theta\right) \neq \mathbf{0}, \quad (27)$$

$$\mathsf{im}(\mathbf{g}(\theta)) \cap \left(\mathcal{C}_y) \cap \mathcal{C}_\theta\right) \neq \mathbf{0}. \quad (28)$$

Field $\mathbf{g}(\theta)$ is a function of θ without singularities if $\theta \neq \pi/2 + k\pi$ with $k \in \mathbb{N}$. For sake of brevity the following field is calculated considering just $\theta = 0$:

$$(\mathbf{g}(\theta))^\dagger = \begin{bmatrix} 0 & 0 & 0 & a(\theta) & 0 & b(\theta) \\ 0 & c(\theta) & 0 & -a(\theta) & 0 & b(\theta) \\ 0 & -c(\theta) & 0 & -a(\theta) & 0 & b(\theta) \end{bmatrix}, \quad (29)$$

where with $(\mathbf{g}(\theta))^\dagger$ the pseudo inverse of field $\mathbf{g}(\theta)$ is indicated. Functions $a(\theta)$, $b(\theta)$ and $c(\theta)$ are functions of the variable θ with $\theta \approx 0$. The following calculation is obtained for $\theta \neq \pi/2 + k\pi$ with $k \in \mathbb{N}$:

$$\mathcal{C}_x \cap \mathcal{C}_y = \mathsf{im}\begin{bmatrix} 0 & 0 & 0 & 0 \\ 1 & 0 & 0 & 0 \\ 0 & 0 & 0 & 0 \\ 0 & -1 & 0 & 0 \\ 0 & 0 & -1 & 0 \\ 0 & 0 & 0 & 1 \end{bmatrix}, \quad (30)$$

$$\mathcal{C}_\theta \cap \mathcal{C}_y = \mathsf{im}\begin{bmatrix} 1 & 0 & 0 & 0 \\ 0 & 1 & 0 & 0 \\ 0 & 0 & 0 & 0 \\ 0 & 0 & 1 & 0 \\ 0 & 0 & 0 & 0 \\ 0 & 0 & 0 & 1 \end{bmatrix}, \quad (31)$$

$$\mathcal{C}_\theta \cap \mathcal{C}x = \mathsf{im}\begin{bmatrix} 0 & 0 & 0 & 0 \\ 1 & 0 & 0 & 0 \\ 0 & 1 & 0 & 0 \\ 0 & 0 & 1 & 0 \\ 0 & 0 & 0 & 0 \\ 0 & 0 & 0 & 1 \end{bmatrix}. \quad (32)$$

The following calculation allow to get the required fields for the decoupling of the mechanical system:

$$\mathbf{T}_\theta(\theta) = (\mathbf{g}(\theta))^\dagger \cdot \mathsf{im}(\mathbf{g}(\theta)) \cap \mathcal{C}_x \cap \mathcal{C}_y, \quad (33)$$

$$\mathbf{T}_x(\theta) = (\mathbf{g}(\theta))^\dagger \cdot \mathsf{im}(\mathbf{g}(\theta)) \cap \mathcal{C}_\theta \cap \mathcal{C}_y, \quad (34)$$

$$\mathbf{T}_y(\theta) = (\mathbf{g}(\theta))^\dagger \cdot \mathsf{im}(\mathbf{g}(\theta)) \cap \mathcal{C}_\theta) \cap \mathcal{C}_x. \quad (35)$$

Adding all 3 T-Fields together we get a new field $\mathbf{T}(\theta)$:

$$\mathbf{T}(\theta) = \mathbf{T}_x(\theta) + \mathbf{T}_y(\theta) + \mathbf{T}_\theta(\theta). \quad (36)$$

Field $\mathbf{T}(\theta)$ can be seen as a preselecting field and the following product realises the mechanical decoupling:

$$\mathcal{B} = \mathsf{im}(\mathbf{g}(\theta)\mathbf{T}(\theta)) = \mathsf{im}\begin{bmatrix} 0 & 0 & 0 \\ 1 & 0 & 0 \\ 0 & 0 & 0 \\ 0 & 1 & 0 \\ 0 & 0 & 0 \\ 0 & 0 & 1 \end{bmatrix}, \quad (37)$$

in which matrix $\mathbf{B}$ can be seen as a resulting input matrix.

IV. On the Functional Controllability of the Robotino

This section is aimed at the analysis of the output functional controllability of Robotino system. As already pointed out, we are interested in controlling motion tracking without transients of error variables. On the whole, in Robotino control, the exact trajectory tracking is an ambitiosous objective and this is particularly emphasized by advanced control tasks recalled in Section I. It is our belief that decoupling should be a basic requirement of force and object–motion control, thus the objective of the control becomes twofold and an effort is made to achieve both decoupling and functional controllability of reachable motions. To attack the problem, the natural approach is to analyze the constrained output controllability idea, cf. [9] and [1], formalized below.

Definition 2: **(Perfect output controllability)** Given the triple $(\mathbf{A}, \mathbf{B}, \mathbf{C})$, the output subspace $\mathcal{L}^i$ is said to be perfect output functionally output functional controllable with respect to i-th derivative and with respect to the subspace of states $\mathcal{F}$ if $\mathcal{L}^i = \mathbf{C}\mathcal{F}$ and, for every initial state $\mathbf{x}_0 \in \mathcal{F}$, it is possible, by means of proper bounded and measurable

control functions, to follow in $\mathcal{L}$ any trajectory arbitrarily given in the class of functions which admit i-th derivative with respect to time, while the state evolves into $\mathcal{F}$.

□

Recall, cf. [9], that the output functional controllability is strictly related to the geometric–type extension of the relative degree for multivariable systems and that each subspace $\mathcal{F}$ satisfying Definition 2 is an $(\mathbf{A}, \mathbf{B})$–controlled invariant.
The following theorem which was demonstrated in [9] and in [1] is reported here below to be applied for the Robotino case.

Theorem 1: (**Output Functional Controllability and Decoupling of the Robotino**) The output subspaces $\mathsf{im}(\mathbf{C}_x)$, $\mathsf{im}(\mathbf{C}_y)$ and $\mathsf{im}(\mathbf{C}_\theta)$ are output functional controllable with respect to the 3^{rd} derivative and with respect to the constrained reachable subspaces $\mathcal{R}_x(\theta)$, $\mathcal{R}_y(\theta)$, and $\mathcal{R}_\theta(\theta)$ respectively. Moreover field $\mathbf{T}(\theta)$ makes the system, with outputs $x(t)$, $y(t)$ and $\theta(t)$ decoupled and output functional controllable.

□

Remark 1: Regarding the functional controllability of rigid–body as object motions, the 3^{rd} order of derivative means that the outputs $x(t)$, $y(t)$ and $\theta(t)$ can perfectly track any desired trajectories $x_d(t)$, $y_d(t)$ and $\theta_d(t)$ which has a piecewise continuous 3^{rd} derivative. This is true for all initial states $\mathbf{x}_o$ in $\mathcal{R}_x(\theta)$, $\mathcal{R}_y(\theta)$, and $\mathcal{R}_\theta(\theta)$ and with piecewise continuous control functions $\mathbf{F}(t)$. Furthermore, it could be easily shown that order 3 of the rigid–body object motions is not due to the particular choice of the subspaces $\mathcal{R}_x(\theta)$, $\mathcal{R}_y(\theta)$, and $\mathcal{R}_\theta(\theta)$ but it is an inherent property of the system. It is related to the relative degree of the relationship between the rigid–body object motion and the DC-Drive input voltage.

□

In the following a fundamental condition is shown, further details in [9].

Projection Condition
Given the system represented as $(\mathbf{A}, \mathbf{B}, \mathbf{C})$. $\mathcal{F}^i$ *is a subspace of functional controllability of the output with respect to the* i*-derivative, if and only if*

$$\mathcal{F}^i \subseteq \mathcal{F}^i \cap \mathcal{Z}_{i-1} + \mathcal{C}, \tag{38}$$

where $\mathcal{Z}^{i-1}$ *is defined in the following way:* $\mathcal{Z}_o = \mathcal{B}$ *and* $\mathcal{Z}_j = \mathcal{B} + \mathbf{A}(\mathcal{Z}_{j-1} \cap \mathcal{F}^i \cap \mathcal{C})$. □

Sketch of the proof considering the Robotino case
It is to be remarked that the Projection Condition states a necessary and sufficient condition for functional controllability of a system. If just the mechanical part of the model is considered, it is possible to show that an output controllability with respect to the second derivative is obtained. In fact, in case $i = 2$, in a generic point $\overline{\mathbf{x}} \in \mathcal{F}^2$ of a generic trajectory, exists, per definition, at least a velocity of state $\dot{\overline{\mathbf{x}}} \in \mathcal{F}^2$. All admissible velocities on $\mathcal{F}^2$ are obtained adding to $\dot{\overline{\mathbf{x}}}$ vectors belonging to subspace $\mathcal{F}^2 \cap \mathcal{B}$. Thus, such a subspace represents the set of all possible velocity variations and $\mathcal{F}^2 \cap \mathcal{B} \cap \mathcal{C}$ represents the set of all velocity variations which are not visible from the output. Being in general

$$\ddot{\mathbf{x}}(t) = \mathbf{A}\dot{\mathbf{x}}(t) + \mathbf{B}\dot{\mathbf{u}}(t), \tag{39}$$

then with a suitable choice of the control $u_1(t) + u_2(t)$, in which $u_1(t)$ is manipulable in its second derivative and such that $\mathbf{B}u_1(t) \in \mathcal{F}^2 \cap \mathcal{B} \cap \mathcal{C}$, and $u_2(t)$ is manipulable in its first derivative and such that $\mathbf{B}u_2(t) \in \mathcal{B}$. Thus, if the trajectory evolves in the following subspace

$$\mathcal{Z}_1 = \mathcal{B} + \mathbf{A}\mathcal{F}^2 \cap \mathcal{B} \cap \mathcal{C}, \tag{40}$$

it is possible to variate the second derivative of it. A trajectory belongs to $\mathcal{F}^2$ if its derivative belongs to $\mathcal{F}^2$ (invariant subspace definition according to [1]) and it is necessary that its variations belong to $\mathcal{Z}_1 \cap \mathcal{F}^2$. If $\mathcal{L}^2$ indicates an output subspace, then $\mathcal{L}^2 = \mathbf{C}\mathcal{F}^2$ is a subspace of output functional controllability with respect to the second derivative if and only if

$$\mathbf{C}\mathcal{F}^2 = \mathbf{C}(\mathcal{F}^2 \cap \mathcal{Z}_1), \tag{41}$$

or

$$\mathcal{F}^2 + \mathcal{C} = \mathbf{C}(\mathcal{F}^2 \cap \mathcal{Z}_1) + \mathcal{C}. \tag{42}$$

□

Remark 2: In other words, subspace $\mathcal{Z}_1$ represents the subspace of all the manipulable trajectories with continuous second derivative. If the trajectory belongs to $\mathcal{Z}_1$, then it is possible to manipulate the first and the second derivatives in $\mathcal{Z}_1$. This can be done by means of proper bounded and measurable control functions. In fact, in so doing it is possible to follow in $\mathcal{L}^2$ any trajectory arbitrarily given in the class of functions which admit 2^{nd} derivative with respect to time, while the state evolves into $\mathcal{F}^2$.

□

Considering again the mechanical system and choosing subspaces $\mathcal{F}_x$, $\mathcal{F}_y$ and $\mathcal{F}_\theta$ as candidate subspaces:

$$\mathcal{F}_x = \mathsf{im}\begin{bmatrix} 1 & 0 \\ 0 & 1 \\ 0 & 0 \\ 0 & 0 \\ 0 & 0 \\ 0 & 0 \end{bmatrix}, \quad \mathcal{F}_y = \mathsf{im}\begin{bmatrix} 0 & 0 \\ 0 & 0 \\ 1 & 0 \\ 0 & 1 \\ 0 & 0 \\ 0 & 0 \end{bmatrix}, \quad \text{and} \tag{43}$$

$$\mathcal{F}_\theta = \mathsf{im}\begin{bmatrix} 0 & 0 \\ 0 & 0 \\ 0 & 0 \\ 0 & 0 \\ 1 & 0 \\ 0 & 1 \end{bmatrix}. \tag{44}$$

It can be shown that the mechanical system with this choice of subspaces can be functionally controllable on trajectories

with continuous 2^{nd} derivatives. In fact, considering that $\mathcal{F}^1 \nsubseteq \mathcal{F}^1 \cap \mathcal{Z}_0 + \mathcal{C}_x$, to be more precise

$$\mathcal{F}_x^1 \cap \mathcal{Z}_0 = \begin{bmatrix} 0 \\ 1 \\ 0 \\ 0 \\ 0 \\ 0 \end{bmatrix}, \tag{45}$$

so the mechanical system is not functional controllable with respect trajectories of the 1^{st} order. Similar results can be obtained for considering the output subspace $\mathsf{im}\mathbf{C}_y$ and $\mathsf{im}\mathbf{C}_\theta$. If the following relation is considered $\mathcal{F}_x^2 \subseteq \mathcal{F}_x^2 \cap \mathcal{Z}_1 + \mathcal{C}_x$, to be more precise

$$\mathcal{Z}_1 = \begin{bmatrix} 0 & 0 & 0 \\ 1 & 0 & 0 \\ 0 & 0 & 0 \\ 0 & 1 & 0 \\ 0 & 0 & 0 \\ 0 & 0 & 1 \end{bmatrix} + \begin{bmatrix} 0 & 1 & 0 & 0 & 0 & 0 \\ 0 & -\frac{k_v}{M} & 0 & 0 & 0 & 0 \\ 0 & 0 & 0 & 1 & 0 & 0 \\ 0 & 0 & 0 & -\frac{k_v}{M} & 0 & 0 \\ 0 & 0 & 0 & 0 & 0 & 1 \\ 0 & 0 & 0 & 0 & 0 & -\frac{k_\theta}{J} \end{bmatrix}.$$

$$\mathsf{im}\begin{bmatrix} 1 & 0 \\ 0 & 1 \\ 0 & 0 \\ 0 & 0 \\ 0 & 0 \\ 0 & 0 \end{bmatrix} \cap \begin{bmatrix} 0 & 0 & 0 \\ 1 & 0 & 0 \\ 0 & 0 & 0 \\ 0 & 1 & 0 \\ 0 & 0 & 0 \\ 0 & 0 & 1 \end{bmatrix} \cap \mathsf{im}\begin{bmatrix} 0 & 0 & 0 \\ 1 & 0 & 0 \\ 0 & 0 & 0 \\ 0 & -1 & 0 \\ 0 & 0 & 0 \\ 0 & 0 & 1 \end{bmatrix} = \mathcal{B}. \tag{46}$$

$$\mathcal{F}_x^2 \cap \mathcal{Z}_1 = \mathcal{F}_x^2. \tag{47}$$

It is possible to see then that equation (41) is satisfied thus also equation (42) is satisfied. Similar results can be obtained for considering the output subspace $\mathsf{im}\mathbf{C}_y$ and $\mathsf{im}\mathbf{C}_\theta$.

Remark 3: Considering relation (42) it is possible to see that functional subspace $\mathcal{F}^2$ consists of the position subspace along trajectory x(t) and its velocity subspace. Moreover, the velocity subspace belongs to $\mathcal{C}_x$. Similar considerations can be obtained considering the output subspace $\mathsf{im}\mathbf{C}_y$ and $\mathsf{im}\mathbf{C}_\theta$. □

Considering the electrical drive which is connected in input to the mechanical one, it can be shown that this system is functionally controllable considering trajectories with continuous 1^{st} derivative. To conclude, considering the cascade structure of the whole system, the Robotino can be functionally controlled considering trajectories with continuous 3^{rd} derivative.

V. Solving Three Decoupled Linear Position MPC Optimization Problems for the Mechanical System

If matrix (3) is observed, it is possible to notice that this matrix is a block matrix and thus represents, as already observed, an internally decoupled system. Considering that together with the preselecting matrix $\mathbf{T}_\theta$ above calculated, it is possible to consider a centralized decoupled model predictive controller as follows. Considering $k = nT_s$ and $k+1 = (n+1)T_s$, where T_s represents the sampling time and $n \in \mathbb{N}$, then

$$u_{mpc}(k) = u_{mpc}(k-1) + \Delta u_{mpc}(k), \tag{48}$$

then the following expression can be obtained

$$\begin{aligned} \mathbf{x}(k+1) &= \mathbf{A}_{(\cdot)_k}\mathbf{x}(k) + \mathbf{B}_{(\cdot)_k}\Big(\Delta u_{mpc}(k) + u_{mpc}(k-1)\Big) \\ y(k) &= \mathbf{H}_{(\cdot)_k}\mathbf{x}(k), \end{aligned} \tag{49}$$

where $\mathbf{A}_{(\cdot)_k}$ represents the discretisation of each block matrix of definition (4) of matrix $\mathbf{A}$, matrix $\mathbf{B}_{(\cdot)_k}$ represents in the same way the discretisation of each block matrix of definition (37) of matrix $\mathbf{B}$, $\mathbf{x}(k)$ is the corresponding discrete part of the state variable and matrix $\mathbf{H}_{(\cdot)_k}$ is the output matrix which determines the position. A general MPC approach with control increments is considered. Using the recursive relation in (48) with a prediction horizon of four the following equation can be obtained:

$$\mathbf{Y}(k) = \mathbf{G}_p\mathbf{x}(k) + \mathbf{F}_{1p}(k)\mathbf{\Delta U}_{mpc}(k) + \mathbf{F}_{2p}u_{mpc}(k-1), \tag{50}$$

where

$$\mathbf{Y}(k) = \begin{bmatrix} \hat{y}(k+1/k) \\ \hat{y}(k+2/k) \\ \hat{y}(k+3/k) \\ \hat{y}(k+4/k) \end{bmatrix}, \quad \mathbf{\Delta U}_{mpc}(k) = \begin{bmatrix} \Delta u_{mpc}(k) \\ \Delta u_{mpc}(k+1) \\ \Delta u_{mpc}(k+2) \\ \Delta u_{mpc}(k+3) \end{bmatrix} \tag{51}$$

and matrices $\mathbf{G}_p$, $\mathbf{F}_{1p}$ and $\mathbf{F}_{2p}$ is given here below:

$$\mathbf{G}_p = \begin{bmatrix} \mathbf{H}_k\mathbf{A}_{(\cdot)_k} \\ \mathbf{H}_k\mathbf{A}_{(\cdot)_k}^2 \\ \mathbf{H}_k\mathbf{A}_{(\cdot)_k}^3 \\ \mathbf{H}_k\mathbf{A}_{(\cdot)_k}^4 \end{bmatrix}, \quad \mathbf{F}_{1p} = \begin{bmatrix} \mathbf{H}_k\mathbf{B}_{(\cdot)_k} & \mathbf{0} & \mathbf{0} & \mathbf{0} \\ \mathbf{H}_k\mathbf{A}_{(\cdot)_k}\mathbf{B}_{(\cdot)_k} & \mathbf{H}_k\mathbf{B}_{(\cdot)_k} & \mathbf{0} & \mathbf{0} \\ \mathbf{H}_k\sum_{i=1}^{2}\left(\mathbf{A}_{(\cdot)_k}^i + \mathbf{I}\right)\mathbf{B}_{(\cdot)_k} & \mathbf{H}_k(\mathbf{A}_{(\cdot)_k} + \mathbf{I})\mathbf{B}_{(\cdot)_k} & \mathbf{H}_k\mathbf{B}_{(\cdot)_k} & \mathbf{0} \\ \mathbf{H}_k\sum_{i=1}^{3}\left(\mathbf{A}_{(\cdot)_k}^i + \mathbf{I}\right)\mathbf{B}_{(\cdot)_k} & \mathbf{H}_k\sum_{i=1}^{2}(\mathbf{A}_{(\cdot)_k}^i + \mathbf{I})\mathbf{B}_{(\cdot)_k} & \mathbf{H}_k(\mathbf{A}_{(\cdot)_k} + \mathbf{I})\mathbf{B}_{(\cdot)_k} & \mathbf{H}_k\mathbf{B}_{(\cdot)_k} \end{bmatrix}. \tag{52}$$

$$\mathbf{F}_{2p} = \begin{bmatrix} \mathbf{H}_k \mathbf{B}_{(\cdot)_k} \\ \mathbf{H}_k \big(\mathbf{A}_{(\cdot)_k} + \mathbf{I}\big)\mathbf{B}_{(\cdot)_k} \\ \mathbf{H}_k \sum_{i=1}^{2} \big(\mathbf{A}^i_{(\cdot)_k} + \mathbf{I}\big)\mathbf{B}_{(\cdot)_k} \\ \mathbf{H}_k \sum_{i=1}^{3} \big(\mathbf{A}^i_{(\cdot)_k} + \mathbf{I}\big)\mathbf{B}_{(\cdot)_k} \end{bmatrix}, \tag{53}$$

If the following performance criterion is assumed,

$$J = \frac{1}{2}\sum_{j=1}^{N} \Big(y_d(k+j) - \hat{y}(k+j)\Big)^{\mathrm{T}} \mathbf{Q}_p \Big(y_d(k+j) - \hat{y}(k+j)\Big) + \sum_{j=1}^{N} \Big(\Delta u_{mpc}(k+j)\Big)^{\mathrm{T}} \cdot \mathbf{R}_p \Delta u_{mpc}(k+j), \tag{54}$$

where $x_d(k+j)$, $j = 1, 2, \ldots, N$ is the position reference trajectory and N the prediction horizon, and $\mathbf{Q}_p$ and $\mathbf{R}_p$ are non-negative definite matrices, then the solution minimizing performance index (54) may be then obtained by solving

$$\frac{\partial J}{\partial \Delta \mathbf{U}_{mpc}} = 0. \tag{55}$$

A direct computation of the vectorial optimal solution may be obtained with

$$\Delta \tilde{\mathbf{U}}_{mpc} = (\mathbf{F}_{1p}^{\mathrm{T}} \mathbf{Q}_p \mathbf{F}_{1p} + \mathbf{R}_p)^{-1} \Big(\mathbf{F}_{1p}^{\mathrm{T}} \mathbf{Q}_p \big(\mathbf{Y}_{d_p}(k) - \mathbf{G}_p x(k) - \mathbf{F}_{2p} u_{mpc}(k-1)\big)\Big), \tag{56}$$

where $\mathbf{Y}_{d_p}(k)$ is the desired output column vector. The component at time "k" of the optimal vector of Eq. (56) is to be considered. Further details concerning this MPC can be found in [12].

VI. Simulation Results

Fig. 3 shows the general setup used for simulation and validation. Using a centralized MPC-controller with the geomatric decoupling approach acting as a pre-control, different trajectories can be tracked. As such the MPC accepts trajectories in horizontal, vertical and angular direction and attempts to direct the Robotino only in the specified direction. Therefor it is possible to move the Robotino along the x-axis without a rotation for example.
In the case presented here a cicular movement was attempted while the angular position was to remain constantly zero. Figure 4 shows a very accurate movements along the desired trajectory which is represented in the tested case by a circle. The circle is realized considering a continous sine and a cosine function on the x and y movements. At all time the angular position of the robot was to remain unchanged at zero and this also has been achieved: As can be observed in Figure 5 the simulated result is so small that it is considered to be numerical errors in the simulation. Additionally it is vital, that the drives are not forced to output more than they can handle, so voltages and currents would have to remain in their respective boundaries. Figure 6 shows that aside from the transients at the start the nominal current of 0.9 Ampere was not exceeded. Further testings suggest that with better reference trajectories this could be avoided.

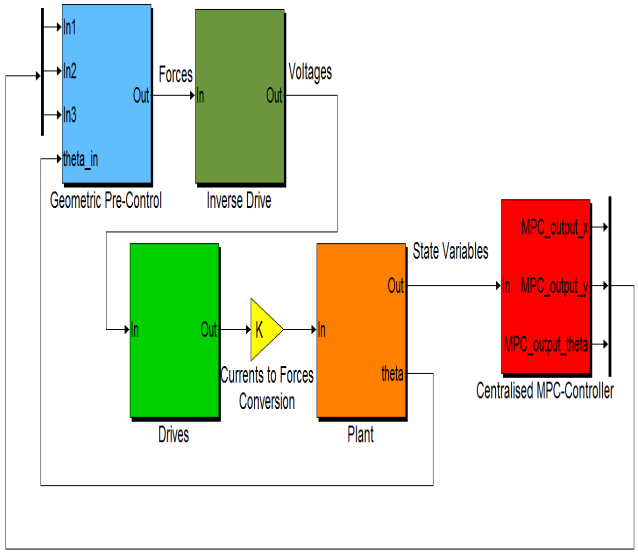

Fig. 3. Block diagram of the control system structure

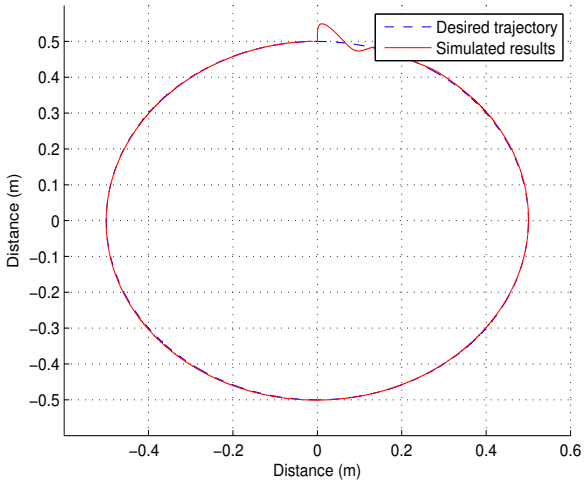

Fig. 4. X-Y-Trajectory of the Robotino

VII. Conclusion

This paper presents a procedure in order to obtain the decoupling functional controllability between horizontal, vertical and angular motions using an geometric approach. Here, the functional decoupling problem is investigated. To achieve a decoupling effect a feedback control law is needed together with a feed-forward regulator. The relevance of the motion functional controllability to Robotino control is justified by the necessity of very fast and very precise loops

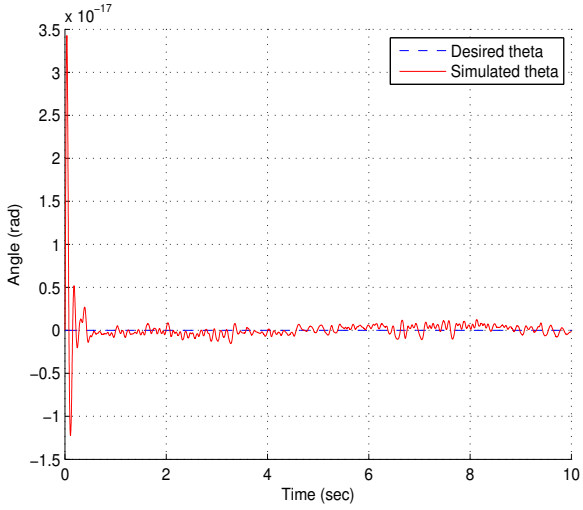

Fig. 5. Change in angular position

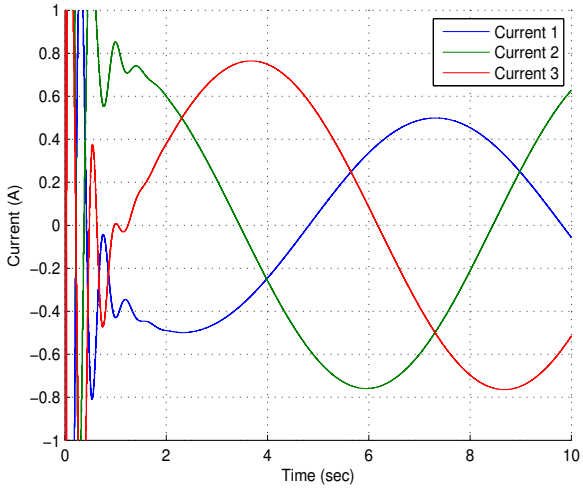

Fig. 6. Currents of the three drives acting the three wheels

of acceleration control counteracting errors in displacements caused by possible disturbance actions. Simulation results are shown to indicate the potential of this approach.

REFERENCES

[1] G. Basile and G. Marro. *Controlled and conditioned invariants in linear system theory*. Prentice Hall, New Jersey, 1992.

[2] A. Isidori. *Nonlinear control Systems: an introduction*. Springer, Berlin, 1989.

[3] W.M. Wonham. *Linear multivariable control: a geometric approach*. Springer, New York, 1979.

[4] P. Mercorelli and D. Prattichizzo. A geometric procedure for robust decoupling control of contact forces in robotic manipulation. *Kybernetika*, 39(4):433–455, 2003.

[5] D. Prattichizzo and P. Mercorelli. On some geometric control properties of active suspension systems. *Kybernetika*, 36(5):549–570, 2000.

[6] P. Mercorelli. Invariant subspace for grasping internal forces and non-interacting force-motion control in robotic manipulation. *Kybernetika*, 48(6):12291249, 2012.

[7] P. Mercorelli. Geometric structures for the parameterization of non-interacting dynamics for multi-body mechanisms. *International Journal of Pure and Applied Mathematics-IJPAM*, 59(3):257–273, 2010.

[8] Y. Yamamoto and X. Yun. Effect of the dynamic interaction on coordinated control of mobile manipulators. *IEEE Transactions on Robotics and Automation*, 12(5):816–824, 1996.

[9] G. Basile and G. Marro. A state space approach to non-interacting controls. *Ricerche di Automatica*, 1(1):68–77, 1970.

[10] W.M. Wonham and A.S. Morse. Decoupling and pole assignment in linear multivariable systems: a geometric approach. *SIAM J. Control*, 8(1):1–18, 1970.

[11] A.S. Morse and W.M. Wonham. Decoupling and pole assignment by dynamic compensation. *SIAM J. Control*, (1):317–337, 1970.

[12] H. Sunan, T.K. Kiong, and L.T. Heng. *Applied Predictive Control*. Springer-Verlag London, Printed in Great Britain, 2002.